EUROPHYSICS LETTERS 1 March 2006

Europhys. Lett., **73** (5), pp. 752–758 (2006)
DOI: 10.1209/epl/i2005-10461-y

Solitary acoustoelectric microwave domain in piezoelectric semiconductors

J. Szeftel[1], P. Leroux-Hugon[2] and G. X. Huang[3]

[1] *ENS Cachan, LPQM - 61 avenue du Président Wilson, 94235 Cachan, France*
[2] *INSP, Campus Boucicaut - 140 rue de Lourmel, 75015 Paris, France*
[3] *Department of Physics, East China Normal University - Shanghai 200062, PRC*

received 18 October 2005; accepted in final form 11 January 2006
published online 25 January 2006

PACS. 72.20.Ht – High-field and nonlinear effects.
PACS. 72.50.+b – Acoustoelectric effects.
PACS. 85.30.Fg – Bulk semiconductor and conductivity oscillation devices (including Hall effect devices, space-charge-limited devices, and Gunn effect devices).

Abstract. – Negative differential conductivity stemming from piezoelectric coupling in semiconductors is shown to arouse a mm wide, high-amplitude acoustoelectric microwave packet moving at sound velocity. Because the electric permittivity is inferred to be renormalized to zero, all properties of this solution (but its width), including its vibrational frequency and amplitude, are shown to be shaped by the nonlinear piezoelectric interaction. An experiment is proposed to check the validity of this analysis. Possible implementation of an acoustoelectric generator is mentioned.

Introduction. – Four decades ago, in the wake of extensive studies of ultrasound amplification [1–4] and related effects [5–7], low-frequency ($\simeq 300\,\mathrm{kHz}$) current oscillations were observed [8–10] in piezoelectric semiconductors (CdS, GaAs, GaSb), undergoing a moderate static electric field ($> 700\,\mathrm{V/cm}$). This effect was characterized by a high-field ($\simeq 3500\,\mathrm{V/cm}$) domain, building up over a low-field ($\simeq 60\,\mathrm{V/cm}$) background and moving throughout the sample at sound velocity. Besides, giant Brillouin scattering [11–13] was reported, which has been accounted for by invoking thermal transverse phonon amplification mediated by the steady current. The frequency associated with the maximum Brillouin scattering cross-section turned out to be smaller than that one corresponding to the largest amplification as inferred from a linear treatment [14]. This discrepancy has been ascribed to the combined effect of phonon absorption and nonlinear parametric processes [13,15,16]. However despite some attempt [9], the high-field domain has remained so far unexplained because the most interesting feature, *i.e.* a large-amplitude ($\simeq 5000\,\mathrm{V/cm}$ peak to peak) microwave field carried along within the solitary domain, has been overlooked due to the low-frequency nature of the detection procedure.

In this letter we explain how the microwave instability ensues from piezoelectricity-induced negative conductivity. The thermal transverse phonons give rise to a direct current flowing in the direction opposed to the Ohmic one, provided the electron drift velocity is larger than the sound velocity [7, 9, 16]. This results into decreased conductivity so that eventually the differential conductivity becomes negative [3, 9, 16], which arouses the solitary wave. We then

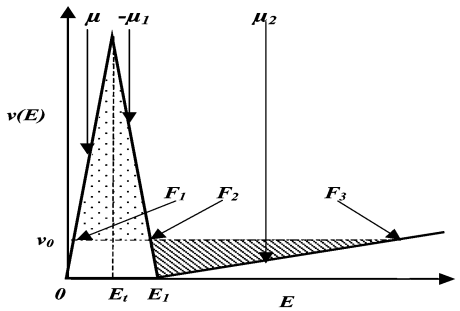

Fig. 1

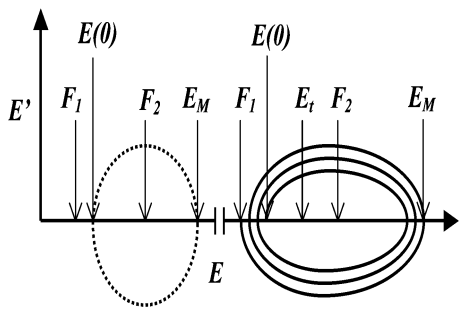

Fig. 2

Fig. 1 – Drift velocity $v(E)$ sketched as a solid curve.

Fig. 2 – Dotted and solid lines refer to the undamped oscillator and solitary wave, respectively. The represented solitary-wave pattern comprises 3 oscillations of $E(z)$.

work out a new master equation by emphasizing the crucial role of the nonlinear piezoelectric coupling (because the linear terms are inferred to lead to a vanishing effective permittivity) and show that this equation does sustain a novel type of solution of spatial extension 1000 times larger than the Gunn oscillation [16, 17, 19], accounting for all observed properties. In particular, the acoustoelectric instability and Brillouin scattering will prove to be unrelated.

The master equation. – In keeping with the observed phenomena [9,16], a one-dimensional sample is considered. An applied static voltage induces the current density $J(x,t)$ (the space coordinate x is such that $0 \leq x \leq L$, where L is the sample length and t stands for time):

$$J = Qv(E) - D_n \frac{\partial Q}{\partial x}, \tag{1}$$

where $Q, v(E), E$ represent, respectively, the density of conduction electrons, their drift velocity and the electric field. The charge density reads $Q = Q_0 + \frac{\partial D}{\partial x}$ while $Q_0, D, \frac{\partial D}{\partial x}$ refer to the equilibrium concentration of conduction electrons, the electric displacement and the space charge density, respectively. The term in eq. (1), proportional to the diffusion constant D_n, is the diffusion current. $v(E)$ is sketched in fig. 1 as linear piecewise for simplicity. In the Ohmic regime ($0 \leq E \leq E_t$), $v(E)$ is equal to μE where μ stands for the electron mobility. $v(E)$ rises to a maximum at the threshold E_t beyond which negative differential conductivity ($\Rightarrow \frac{\mathrm{d}v(E)}{\mathrm{d}E} = -\mu_1 < 0$) sets in over the range $E \in [E_t, E_1]$. Actually, we have checked that thermal transverse acoustic phonons of low frequency ($\omega_\varphi < 10\,\mathrm{GHz}$) induce via linear piezoelectric coupling [14] E and D components $\propto \cos(\omega_\varphi t)$ so that the nonlinear term $\frac{\partial D}{\partial x}\mu E$ in eq. (1) gives rise to a negative direct current, growing with the local electric field and acoustic power and strong enough to bring about $\frac{\mathrm{d}v(E)}{\mathrm{d}E} < 0$. As the ratio of the acoustoelectric current to the Ohmic one $Q_0 \mu E$ is found to decrease with $E > E_t$, $v(E)$ eventually increases for $E > E_1$ ($\Rightarrow \frac{\mathrm{d}v(E)}{\mathrm{d}E} = \mu_2 > 0$). An accurate calculation of $v(E)$ in fig. 1 is beyond the purview of this work because it involves a score of complicated nonlinear effects [15]. All solitary-wave patterns presented below have been worked out with $Q_0 = 1.28 \times 10^{-4}\,\mathrm{C/cm^3}$, $\mu = 6000\,\mathrm{cm^2/(V \times s)}$, which corresponds to a GaAs sample wherein acoustoelectric oscillations were observed [10].

Taking advantage of the charge conservation identity $\frac{\partial J}{\partial x} + \frac{\partial Q}{\partial t} = 0$ in eq. (1) yields

$$\frac{\partial}{\partial x}\left(\left(Q_0 + \frac{\partial D}{\partial x}\right)v(E) - D_n \frac{\partial^2 D}{\partial x^2} + \frac{\partial D}{\partial t}\right) = 0. \tag{2}$$

As the oscillating wave packet has been seen to travel at constant velocity without undergoing any deformation, a solitary solution of eq. (2) should be sought. Thus we replace (x,t) by $z = x - v_s t$, where v_s refers to the propagation velocity of the solitary wave. Equation (2) is recast as

$$D_n D'' = Q_0 \left(v(E) - v_0\right) + D' \left(v(E) - v_s\right), \tag{3}$$

where $D' = \frac{\mathrm{d}D}{\mathrm{d}z}, D'' = \frac{\mathrm{d}^2 D}{\mathrm{d}z^2}$ and the integration constant v_0 has the dimension of a velocity.

The elastic strain $S = \frac{\partial u}{\partial x}$ and the electric field E are coupled together via piezoelectricity,

$$T = cS - eE + f_T(S,E), \qquad D = eS + \epsilon E + f_D(S,E), \tag{4}$$

where T, c, e, ϵ refer [14] to the stress field, elastic, piezoelectric constants and electric permittivity, respectively. $f_T(S,E)$, $f_D(S,E)$ represent the second-order contributions [4, 13, 15] to the Taylor expansions of T, D with respect to S, E which will prove uttermost instrumental in shaping all features of the acoustoelectric solitary wave.

Using Newton's law, $\rho \frac{\partial^2 u}{\partial t^2} = \frac{\partial T}{\partial x}$ (ρ stands for the specific mass), yields $T - \rho v_s^2 S = 0$ after replacing (x,t) by $z = x - v_s t$ and integrating over z. Taking advantage of eqs. (4) leads to

$$S = \frac{e}{c - \rho v_s^2} E + \alpha_S E^2, \qquad D = \epsilon^\star E + \alpha_D E^2, \qquad \epsilon^\star = \epsilon + \frac{e^2}{c - \rho v_s^2},$$

where $\epsilon^\star$ is an effective electric permittivity. The explicit dependence of α_S, α_D upon $\frac{\partial^2 f_X}{\partial E^2}$, $\frac{\partial^2 f_X}{\partial S \partial E}$, $\frac{\partial^2 f_X}{\partial S^2}$ where $X = T,\ D$ is of little interest because those partial second derivatives are not known. Therefore α_S, α_D will be rather dealt with as disposable parameters hereafter.

The solitary wave was observed [8–10] to travel at the transverse sound velocity $v_s = \sqrt{\frac{c}{\rho}(1 + \frac{e^2}{\epsilon c})}$. The latter has been obtained as a by-product of the dispersion $\omega_\varphi(k)$ of acoustoelectric plane waves, worked out by linearizing eq. (2) as done elsewhere [14]. Consequently, it comes $\epsilon^\star = 0$. Likewise all our attempts to find a *wide* ($\approx 1\,\mathrm{mm}$) solitary solution of eq. (3) with $\frac{\epsilon^\star}{\epsilon} > 10^{-9}$ have failed. Thus, thanks to $\epsilon^\star = 0$, eq. (3) is recast as

$$E'' = Q_1 \frac{v(E) - v_0}{E} + \frac{E'}{D_n} \left(v(E) - v_s\right) - \frac{(E')^2}{E}, \tag{5}$$

where $E' = \frac{\mathrm{d}E}{\mathrm{d}z}, E'' = \frac{\mathrm{d}^2 E}{\mathrm{d}z^2}$, $Q_1 = \frac{Q_0}{2\alpha_D D_n}$. The nonlinear second-order differential equation in eq. (5) is the master equation describing the motion of the solitary wave.

The solitary wave. – In the (E, E') representation depicted in fig. 2, eq. (5) has three fixed points at $(E = F_{i=1,2,3}, E' = 0)$ as due to $v(F_i) = v_0$ (see fig. 1) $E(z) = F_{i=1,2,3}, \forall z$ are solutions of eq. (5). F_1, F_3 are stable because of $\frac{\mathrm{d}v}{\mathrm{d}E}(F_{i=1,3}) > 0$ and pertain to a sample flowed through by a constant current ($= Q_0 v_0$).

Conversely, an oscillatory solution of eq. (5) may arise around F_2 thanks to negative differential conductivity [17] ($\frac{\mathrm{d}v}{\mathrm{d}E}(F_2) < 0$). In principle, were it not for the terms including E' in eq. (5), the corresponding trajectory would be closed (see the dotted curve in fig. 2) as expected for an undamped oscillator. Therefore integrating eq. (5) with initial conditions $E(z=0) > F_1, E'(0) = 0$ should yield $E(z)$ periodic all over the range $z \in [-\infty, +\infty]$ and oscillating between a minimum value $E(0)$ and a maximum one E_M (F_1 is never reached) such that $F_2 < E_M \leq F_3$, related by $\int_{E(0)}^{E_M} \frac{v(E) - v_0}{E} \mathrm{d}E = 0$. As a consequence of the equal area rule [18], a net restoring force is secured only if the characteristic curve in fig. 1 comprises a $\frac{\mathrm{d}v}{\mathrm{d}E} < 0$ section and the dashed area in fig. 1 is sufficiently large with respect to the dotted

one, which sets a lower bound v_m for v_0 (in case $v_0 = v_m$, it comes $E_M = F_3$). Assigning $E_M \approx 5000\,\mathrm{V/cm}$ as inferred from experiments [10] and fulfilling the existence condition for the restoring force has enabled us to ascribe to μ_1, μ_2 the values used in our calculations. The frequency is obtained through a double integration to read

$$\omega_u = \pi v_s \left(\int_{E(0)}^{E_M} \frac{\mathrm{d}E}{\sqrt{2Q_1 \int_{E(0)}^{E} \frac{v(y)-v_0}{y}\mathrm{d}y}} \right)^{-1}.$$

The term $\propto (E')^2$ in eq. (5) acts as an additional restoring force for E near E_M, whence E_M is decreased and the frequency is shifted up to $\omega > \omega_u$. However the damping term $\propto E'$ causes the E, E' trajectory to be *no longer closed*, thereby allowing for a many-oscillation solitary wave (see the solid line in fig. 2) with the lowest (largest) E value within each oscillation decreasing (increasing) from $E(0)$ down to F_1 (up to E_M). At last, note that $E(0) > F_1$ is by all means needed since eq. (5) could sustain only a *single*-oscillation solution, similar to the Gunn effect, in case $E(0) = F_1$ (note also $v_0 \neq v_s$ as opposed to $v_0 = v_s$ required for the Gunn effect [16, 17, 19]).

First, eq. (5) has been solved for $E(z \in [0, l]) > 0$ ($\Rightarrow S(E) < 0$), where $l < L$ is the width of the high-field domain. Besides, $E > 0$ entails $\alpha_D > 0$ in order to ensure a restoring force. Assigning v_0 $\left(\Rightarrow F_1 = \frac{v_0}{\mu}\right)$ has enabled us to integrate eq. (5) from $z = 0$ with the initial conditions $E(0) > F_1, E'(0) = 0$. The final values $E(l), E'(l)$ at $z = l$ depend then only on $v_0, E(0)$. As we want $E(l)$ close to F_1 and $E(z \to \infty) \to F_1$ because the fixed point $(E = F_1, E' = 0)$ in fig. 2 can only be reached asymptotically for $z \to \infty$, it suffices, for $z > l$, to integrate eq. (5) linearized [16, 17] around F_1, which reads

$$E'' = \frac{Q_1 \mu^2}{v_0} E + \frac{v_0 - v_s}{D_n} E'. \tag{6}$$

Thus it comes

$$E(z > l) = (E(l) - F_1)\, e^{\kappa(z-l)} + F_1, \qquad \kappa = \frac{\frac{v_0 - v_s}{D_n} - \sqrt{\left(\frac{v_0 - v_s}{D_n}\right)^2 + \frac{4Q_1\mu^2}{v_0}}}{2} < 0.$$

For $E(z), E'(z)$ to remain continuous at $z = l$, two matching conditions must be satisfied:

$$\frac{E(l)}{F_1} - 1 = \eta \ll 1, \qquad \frac{E'(l)}{E(l) - F_1} = \kappa. \tag{7}$$

Finally, integrating eq. (5) over $[0, L]$ is tantamount to solving eqs. (7) for the unknowns v_0, $E(0)$ (remember that $E(l)$, $E'(l)$ are functions of v_0, $E(0)$). This has been done as follows: i) integrate eq. (5) from $z = 0$ up to $z = l$ defined by $E(l) = F_1$; ii) solve eqs. (7) for that l value kept fixed and $\eta = 0.01$ by using Newton's method to yield the acoustoelectric solitary-wave patterns pictured in figs. 3, 4. The assignment $D_n = 1000\,\mathrm{cm^2/s}$ has been estimated from the literature [20], while taking into account the hot-electron temperature induced by the strong E field. For simplicity, $S(z)$ has been worked out with $\alpha_S = 0$.

The solitary-wave width l is not an intrinsic property of eq. (5). Hence defining the mean E value within the solitary wave as $E_o = \frac{\int_0^l E(z)\mathrm{d}z}{l}$, the time behavior of l is assessed by requiring that integrating E over the sample length L equal the applied voltage U:

$$U = \int_L^0 E(z)\mathrm{d}z = -\left(E(0)v_s t + E_o l + F_1(L - v_s t - l)\right). \tag{8}$$

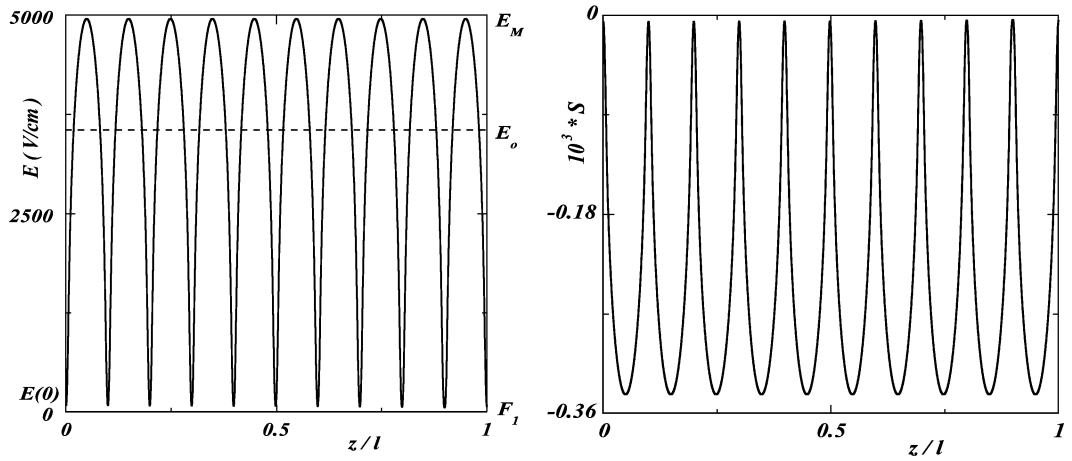

Fig. 3 – Plots of $E(z), S(z)$ (solid line) and E_o (dashed line) reckoned with $Q_1 = 10^9\,\mathrm{V}^2 \times \mathrm{s/cm}^5$, $l = 60\mu \Rightarrow \frac{v_0}{v_s} - 1 = 5 \times 10^{-5}$, $E(0) - F_1 = 31\,\mathrm{V/cm}$, $\kappa^{-1} = -305\,\text{Å}$, $E_M = 4957\,\mathrm{V/cm}$, $E_o = 3555\,\mathrm{V/cm}$, $\omega = 3.5\,\mathrm{GHz}$.

As $E(0)$, E_o, F_1 depend on a single parameter l, solving eq. (8) provides indeed l *vs.* time t (the small difference $(E(z > v_s t + l) - F_1) < \eta F_1$ has been neglected in eq. (8), which entails that $\int_{v_s t+l}^{L} E(z)\mathrm{d}z = F_1(L - v_s t - l)$).

Discussion. – The observed solitary wave [8–10] consists of a large field domain moving above a weak-field background, $= E(0)$ or F_1 behind and ahead of the solitary wave, respectively. Actually, the low-frequency detection method was bound to miss the momentous property that the solitary wave carries a high-frequency ($= \omega$) wave packet so that only its mean value E_o was observed. The applied field $E_a = \frac{|U|}{L} > E_t$ induces an Ohmic current

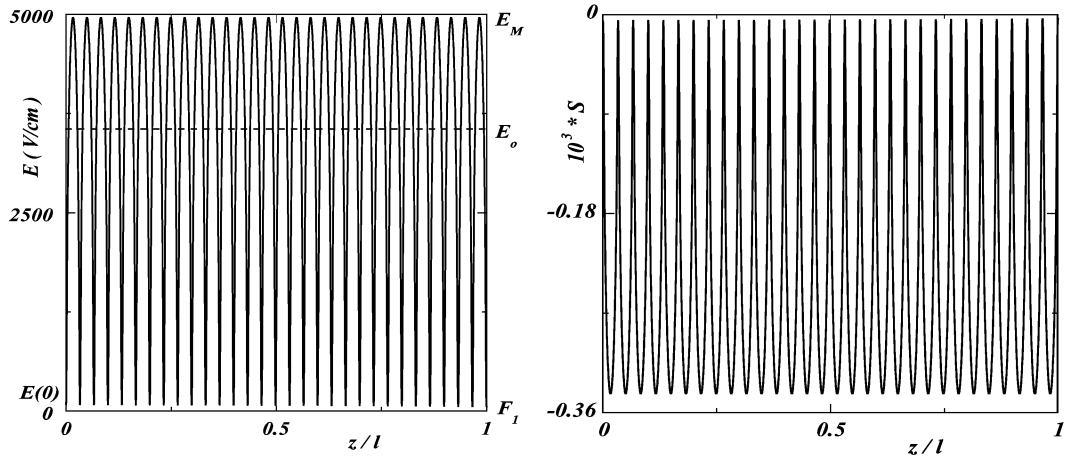

Fig. 4 – Plots of $E(z), S(z)$ (solid line) and E_o (dashed line) reckoned with $Q_1 = 10^{10}\,\mathrm{V}^2 \times \mathrm{s/cm}^5$, $l = 57\mu \Rightarrow \frac{v_0}{v_s} - 1 = 5 \times 10^{-5}$, $E(0) - F_1 = 31\,\mathrm{V/cm}$, $\kappa^{-1} = -96\,\text{Å}$, $E_M = 4957\,\mathrm{V/cm}$, $E_o = 3556\,\mathrm{V/cm}$, $\omega = 11\,\mathrm{GHz}$.

which starts amplifying the thermal transverse phonon field. This contributes to reducing the differential conductivity [9] till it becomes negative, which excites the acoustoelectric solitary wave to arise. Phonon amplification, enhanced by the high E_o value, saturates [5] eventually after $\approx 1\,\mu$s [8] so that $v(E)$ reaches its final shape as sketched in fig. 1. During the solitary-wave building process, $l(t)$ is given by solving eq. (8), keeping in mind that $E(0), E_o, F_1$ depend solely on l and are obtained by integrating eq. (5) under the matching conditions in eqs. (7) while using the characteric curve $v(E)$ available at t.

Given [10] $L = 1\,$cm and $F_1 \ll E_a$, a value of l in the mm range is required to satisfy eq. (8) in keeping with observation. However, the damping term $\propto E'$ in eq. (5) limits l down to much smaller values ($\approx 3\mu$) unless v_0 is pinned onto v_s. Indeed l decreases very steeply with v_0 drawing apart from v_s as $\delta v = \frac{v_0}{v_s} - 1 = 3 \times 10^{-6}$, 8×10^{-5} correspond, respectively, to $l = 948\mu$, 36μ (l behaves fairly well like δv^{-1}). Thence increasing E_a further causes the solitary-wave width l to grow while $E_o, F_1 = \frac{v_s}{\mu}$ remain unaltered in agreement with observation [8–10].

For $0 < t < 1\,\mu$s, that is until the high-field domain has grown significantly, the current keeps its initial Ohmic value $= Q_0 \mu E_a$. Thereafter it drops down to the low-field, E_a-*independent* value $Q_0 \mu F_1 (= Q_0 v_s)$ and oscillates between these limits with the time period $\frac{L}{v_s} (\approx 3\,\mu$s) needed for the solitary wave to travel throughout the sample in accordance with observation [10]. As the time required for the $\frac{\mathrm{d}v(E)}{\mathrm{d}E} < 0$ domain to grow must be in any case shorter than $\frac{L}{v_s}$, the threshold E_t should increase with decreasing L as indeed observed [10] because phonon amplification increases with E_a, which compensates for shorter L. At last these current oscillations turn out to be physically unrelated to another kind of low-frequency plasma-like oscillations [6, 21], the period of which is anyhow $\neq \frac{L}{v_s}$.

The difference $E(0) - F_1 > 0$ has been observed [10]. The solitary-wave width l increases with $E(0) - F_1$ but it does so *stepwise* because eqs. (7) can be satisfied only if $l = n\lambda$ (see figs. 3, 4), where n is an integer and $\lambda = 2\pi \frac{v_s}{\omega}$ refers to the wavelength of the wave packet. After the full-fledged solitary wave has grown for $t > 1\,\mu$s, $E(0) - F_1$ is responsible for l decreasing with t. Equation (8) provides the shrinking rate as $\dot{l} = v_s \frac{F_1 - E(0)}{E_o}$. Then using the experimental data for $F_1, E(0), E_o$ yields a total decrease $\frac{\mathrm{d}l}{l} < 5\%$ for $L = 1\,$cm, which lies within experimental accuracy.

As expected for a nonlinear oscillator, the vibrational pattern bears no resemblance with a sine wave, which results into $E_o \neq \frac{F_1 + E_M}{2}$. Unlike l, the frequency ω is an intrinsic property of eq. (5) and behaves like $\sqrt{Q_1}$ (compare fig. 3 with fig. 4). As a reliable value for α_D entering the definition of Q_1 is lacking, the ω value cannot be predicted. To that end we suggest two independent experiments, which could permit to confirm the existence of the acoustoelectric solitary wave. The longitudinal electric wave could excite an electromagnetic field in a microwave cavity tuned at ω and properly coupled to the sample, whereas the transverse strain wave should be all the more prone to detection by Brillouin scattering since its vibrational amplitude is large (up to 4×10^{-4} in figs. 3, 4). Measuring the *same* frequency ω for the electromagnetic wave *and* the Brillouin scattering signal would bring compelling evidence for the validity of this analysis. Nevertheless, no narrow signal has been reported in Brillouin scattering experiments [11–13]. This failure might be due to two reasons. Either the narrow peak at ω has been overlooked because it remained buried inside the broad ($\approx$ 0.5 GHz) incoherent contribution of thermal phonons as the outgoing light frequency was not analysed in the published measurements [11–13], or $\omega > \omega_M = 2\omega_l \frac{v_s}{c}$ where ω_M refers to the largest possible phonon frequency to be detected in a Brillouin scattering experiment using ingoing light of frequency ω_l and velocity c. Performing the experiment with larger ω_l, while analysing the scattered light frequency with high resolution, would then be needed. It

is also noteworthy that these proposed experiments lay out the principle of a powerful and versatile acoustoelectric generator in the microwave range.

Conclusion. – The long-standing problem of the high-field domain, travelling at sound velocity in piezoelectric semiconductors, and low-frequency associated current oscillations has been settled in terms of an acoustoelectric solitary wave comprising thousands of coherent microwave oscillations of very large amplitude. All experimental features have been accounted for. This instability stems from negative differential conductivity showing up in the current-voltage characteristic. It is entirely governed by nonlinear piezoelectric coupling because the effective electric permittivity has been shown to vanish. The large field E_o enhances the Brillouin scattering [11–13] by amplifying the thermal phonons [14] within the solitary wave. Otherwise the two effects are unrelated even though the nonlinear piezoelectric effect proves instrumental in both cases. In particular the incoherent phonon frequency corresponding to maximum Brillouin scattering and the coherent frequency ω of the acoustoelectric solitary wave should be quite different. Finally, since the microwave frequency ω is an intrinsic property of the equation of motion whereas the solitary wave width l is not, the whole physical picture shows up outright opposed to the Gunn effect [16, 17, 19].

* * *

We are indebted to E. Bringuier for his critical reading of the manuscript and to I. Ledoux and J. Zyss for providing encouragement. One of us (GXH) is grateful to Université Paris 7 for a visiting grant.

REFERENCES

[1] Hutson A. R., McFee J. H. and White D. L., *Phys. Rev. Lett.*, **7** (1961) 237.
[2] Spector H. N., *Phys. Rev.*, **127** (1962) 1084.
[3] McFee J. H., *J. Appl. Phys.*, **34** (1963) 1548.
[4] Tell B., *Phys. Rev.*, **136** (1964) A772.
[5] Smith R., *Phys. Rev. Lett.*, **9** (1962) 87.
[6] Kroger H., Prohofsky E. W. and Carleton H. R., *Phys. Rev. Lett.*, **12** (1964) 555.
[7] McFee J. H. and Tien P. K., *J. Appl. Phys.*, **37** (1966) 2754.
[8] Sliva P. O. and Bray R., *Phys. Rev. Lett.*, **14** (1965) 372.
[9] Haydl W. H., Harker K. and Quate C. F., *J. Appl. Phys.*, **38** (1967) 4295.
[10] Leroux-Hugon P., *Phys. Status Solidi*, **31** (1969) 331.
[11] Zucker J. and Zemon S., *Appl. Phys. Lett.*, **9** (1966) 398.
[12] Chartier G., Koster A. and Leroux-Hugon P., *Phys. Lett. A*, **29** (1969) 379.
[13] Palik E. D. and Bray R., *Phys. Rev. B*, **3** (1971) 3302.
[14] White D. L., *J. Appl. Phys.*, **33** (1962) 2547.
[15] Economou J. E. and Spector H. N., *Phys. Rev. B*, **18** (1978) 5578.
[16] Ridley B. K., *Quantum Processes in Semiconductors* (Clarendon, Oxford) 1999.
[17] Knight B. and Peterson G., *Phys. Rev.*, **155** (1967) 393.
[18] Schöll E. and Landsberg P. T., *Z. Phys. B*, **72** (1988) 515.
[19] Büttiker M. and Thomas H., *Solid State Electron.*, **21** (1978) 95.
[20] Reggiani L., *Hot Electron Transport in Semiconductors* (Springer, Berlin) 1985.
[21] Prohofsky E. W., *Phys. Rev.*, **136** (1964) A1731.